

Analyzing Effects of Stringlines on Initial Smoothness of Concrete Pavements

By

Bernard Igbafen Izevbekhai, P.E.

B.Eng. Hons Civil, University Of Benin, Benin City Nigeria 1983

M.Eng. Civil/ Structural Eng University of Benin, Benin City, Nigeria 1987

MS Infrastructure Systems Engineering, University of Minnesota

Center for the Development of Technological Leadership. 2004

Being a Discussion of the Paper Titled
“Stringline Effects on Concrete Pavement Construction”

November 2008

Abstract

This reviews the paper titled “Effects of stringline on Concrete Pavement Construction, Published by the Transportation Research Journal, Transportation Research Record Issue Number 1900 of 2000. The paper authors discussed traditional slip form paving construction in which a sensor in contact with the stringline determines the finished surface. These stringlines are subject to catenaries and survey errors in regular paving. Additionally they are subject to errors due to chord effects that occur when stringline paving is done on a vertical curve.

Reviewer summarizes the paper, elucidates the major ride quality metrics and accentuates the process of addition of profilograms mentioned by authors. Reviewer further discusses a case study of a classic pavement project that exhibited chatter phenomena to systematically accentuate how stringlines, joint intervals, warp and curl as well as their synergy influence the measured ride quality. The International Roughness Index (IRI) profilograms for the component dominant wavelengths are fitted in a curve to determine correlation to the measured IRI first in the spatial and next in the spectral domain.

Fourier Transform Moduli for component dominant wavelengths were more correlated to that of the measured frequency than the IRI in the spatial domain. The stringline effect were also validated although the paper made little reference to other paving features of equal importance and post pavement built-in warp-and-curl that are of equal and occasionally greater relevance to ride quality.

1) INTRODUCTION

The Paper under review was written Authors Rasmussen, R.O; Karamihas, S.K; Cape, W.R., Chang, G.K., and Guntert, R.M. titled “**Stringline Effects on Concrete Pavement Construction**” is being reviewed. The Paper is hereinafter referred to as the paper and the authors (Rasmussen et al) are herein after referred to as the Authors and for avoidance of doubt, the latter term is not used for the reviewer. Instead the term “review and reviewer” are reserved for this exercise.

Objectives of the Review

- This review primarily accentuates intrinsic issues implicit in the paper. It therefore clearly defines the terms used, expatiates on the paving practices and use of stringlines, enunciating ride quality is actually affected by stringlines.
- It examines other studies germane to the effect of stringlines on ride quality and identifies and discusses relevant areas not covered by authors that elucidate authors’ objectives
- The review discusses a case study of Minnesota Department of Transportation (Mn/DOT) Highway 59 project, a classic case of “Chatter Phenomena” caused by loose stringlines. The review elucidates the spectral content in US Highway 59 project in Morris Minnesota caused by stringlines, joints and synergistic effects of both.
- It consequently advocates a study of Pavement Surface Characteristics in the frequency domain (in preference to or in addition to the spatial domain) towards a better understanding of causative and associative parameters of pavement smoothness.

2) SUMMARY OF THE PAPER

The paper identifies and discusses the use of stringlines as a sensor guide for establishing the finished surface of a concrete paving. Authors (1) noted how the current effort of States and Industry towards smoother pavements and better measurement techniques and metrics had resulted in some states transitioning to the International Roughness Index (IRI). Hitherto most states used the Profile Index (PI) as the metric for pavement smoothness. Authors had neither defined IRI and PI nor mentioned the difference in the response spectra or multiplier algorithm of each of these metrics. According to authors (1) stringlines were introduced to improve pavement smoothness by sensing a stringline to a remarkable degree of precision. This is arguably counterproductive.

The paper identified 3 unique effects of stringlines as

- The chord effect,
- The sag effect and
- Survey errors

They (1) noted that of the 3, survey errors were the most pronounced. Chord effect is explained as the outline of a chord instead of a smooth curve that should normally characterize a vertical curve. If the radius is very large and the stringline support interval is small, chord effect error is minimized. When the radius is large and the stringline support interval is large, there will be severe errors in the profile due to the chord effect. The chord effect is idealized with a system if cable supports joined end to end along a vertical curve and not maintaining the required curvature but a system of chords joined end to

end. The sag effect is caused by tension in the chord that is insufficient to render the string horizontal. The resulting sag profile is dependent on the actual tension at the ends of the stringing process. The survey effect is idealized in terms of a normally distributed set of deviations from the actual nodal points of the stringline set up.

The paper goes further to quantify the effect of stringlines in terms of the percentage increase in roughness due to the already identified causes. Authors then proceeded to demonstrate the effect of the various error sources to quantify and compare their effect on pseudo randomly generated profiles and vertical curves. They (1) generated pseudo random profiles with the procedure prescribed in Appendix E NCHRP 353. This procedure integrates a series of random slopes generated by the equation

$$\text{Slope} = 0 + z(\mathbf{R}) + \sqrt{(\mathbf{G}_s/2\Delta)} \dots \dots \dots 2.1$$

Where z = Inverse of the normal Cumulative distribution based on R

R = A probability number between 0 and 1 dependent on the inverse of the normal cumulative distribution

G_s = White Noise amplitude in ft (m)/cycle chosen as

Δ = Step size in ft or m... chosen as 0.5ft

They consequently generated the vertical curves with the equation

$$E_1 = g_1x + (g_2 - g_1)x^2/2L \dots \dots \dots 2.2$$

Where g_1 = Starting Slope of the vertical curve

E_1 = Initial datum reference for the beginning of the vertical curve

x = Station with respect to the Start of vertical curve

L = Length of curve

Authors superimposed the randomly generated profile on the vertical curve. The curvature of the vertical curve and its length are outside of the range that will cause huge vertical acceleration on the quarter car. The authors thus obtained IRI values that are similar to that of the random profile on a horizontal surface. The catenary due to stringlines was imposed on the vertical curve. The feature was idealized in a format of discontinuous straight lines connected at every 25ft interval. Thereafter, the resulting profile was subjected to the IRI algorithm through a process that is later explained in this review and IRI values were obtained for various corresponding values of g_1 and g_2 . This resulted in a family of values proven to be sensitive to $g_2 - g_1$. Evidently, the higher the value of $|g_2 - g_1|$, the higher the percentage increase in IRI. Respective g_1 and g_2 values of 0 resulted in zero increase in IRI from the smooth vertical curve and respective 0 and 2 resulted in a 5% increase compared to -8 and 8% that resulted in a 171% increase in IRI. It must be noted that the corresponding increase in Ride number was not that significant, not because of scaling difference but because of the dissimilar sensitivity range and gain algorithms (6) for the chosen metric.

The process of addition of profilograms already discussed under chord effect was replicated in the examination of sag effect. Authors also idealized the sag effect by imposing various sag profiles on a

vertical curve and computed the sensitivity of the IRI to these deviations from the curve. Percentage increase in IRI ranged from 0 due to zero sag to 368 % increase in IRI due to an inch sag. To establish the sag profile the sag was computed on the basis of the tension in the string measured.

To quantify the effect of Survey errors, authors generated errors of various standard deviations (SD) from the stringline survey data. To build the factorial, authors generated survey errors in the nodes (stringline supports) in a normal distribution ranging from zero to 0.5 inch with stringline stake interval ranging from 10 to 50 ft. Corresponding IRI ranged from 0 to 383 %.

The paper limits application of these results to systems with single lasers and recognizes unstable foundation wind effects, moisture and temperature changes are responsible for loose stringlines. They also itemized other sources of errors including knot effect, interference effect, foundation effect and wand lift effect.

Although authors referenced other sources of Stringline errors, reviewer observes the following are equally impertinent sources of error.

- **Temperature variation during placement of the Concrete pavement.** The inspectors try to tighten stringlines just before paving and when slackness is observed during paving. Unfortunately it is counterproductive to make adjustments on the stringline when paving had already begun. This is because the surfaces paved after adjustment are in a different stringline setting from the previous segments, thus causing unwarranted kinks in the profile.
- **Oversensitive Stringlines.** Contractors in have alluded to the fact that over-sensitivity of the traveling sensor is counterproductive. For instance, an over sensitive sensor, is adversely affected by the enclosure of the stringline at the support that the sensor interprets as a bump.

3 STRINGLINES IN PAVEMENT CONSTRUCTION

Various vehicles respond to various surface profiles according to their natural frequencies, their sprung masses, spring constants and dashpot constants. Although the international roughness index is a standard measure of ride quality, the measurement is only as good as the degree to which the equipment or ride algorithm responds to the preponderant frequency. The international roughness index is designed to be more sensitive to certain frequencies than others in order to represent how the rider feels. In addition to amplified response of the quarter car to certain frequencies, errors resulting from any deviation from the smooth profile are only predictable to the degree of response of the quarter car algorithm to that profile and the deviation from it.

In consequence when errors due to the paving operations are introduced to the pavement, features certain wavelengths are amplified or attenuation of depending on where a wavelength or frequency fits in the IRI multiplier shown above as above. To understand the concept of IRI multiplier, the basic ride (or roughness) metric deserves a good definition.

The International Roughness index has been variously defined from the simple description of what the name implies (a roughness Index) to the definition in the frequency domain. The international roughness index has been defined (1) as the average rectified velocity (ARV) of the Slope Power Spectrum Density of the profilogram. This definition recognizes implicitly the ramification of

profilograms into various frequencies and amplitudes from which a slope, deflection or vertical acceleration PSD can be plotted. The Slope PSD, Plotted against wavelength (or wave number or frequency) has the dimension of ft/ cycle while the elevation PSD has the dimension of ft²-ft/Cycle. The IRI can therefore be graphically obtained from the Slope PSD. This is a cumbersome process that software such as FHWA ProVAL and UMTRI Roadruf have facilitated. A ride profile can consequently be idealized by Fourier transform or wavelet analysis but the latter 2 may not eliminate the harmonic effects as ProVAL and Road RUF would. Alternately the transform algorithm may be used in the computation as shown in equations 3.4 and 3.5.

Izevbekhai B.I. (2) discussed the effect of texture and joints on pavement roughness in his thesis titled Optimization of Pavement Smoothness and Surface Texturing in Pavement Infrastructure at Center for the Development of Technological Leadership (CDTL) University of Minnesota 2004. The thesis was based on some test sections created in US Highway 212 in Bird Island. The Test sections were made of adjacent yet concurrently finished segments that compared the textured finish to the untextured finish. Results showed that joints and texture did contribute to the computed IRI. Additionally the thesis discussed the friction-ride paradox and proposed an algorithm for incentives and penalties for good and poor ride respectively. In retrospect, the sections were not examined for unusual hot spots associated with string lines.

Karamihas and Sayers. (3) Little book of Profiling discussed the fundamentals of ride measurement and defined many filters particularly “blanking bands” used in the PI metric but do not apply to IRI. Smith K.L, Smith, K.D., Evans L.D., Hoerner, T.E., Darter M.I. in their report “Smoothness Specification for Pavements” Final Report NCHRP 1-31 March 1997 discussed the effect of initial ride quality of pavement performance concluded from nationwide data that pavements with initial high smoothness remain smooth. This is a useful performance predictor re-enacting the fact that initial ride quality is important in pavement practice.

Wilde W. J., Izevbekhai, B.I., and Krause, M.H. compared Profile Index and International Roughness Index in Payment of Incentives in Pavement Construction (TRB 2007) Transportation Research Records, discussed the various effects of paving activities and pavement joint spacing on IRI and PI. In their paper, (3) they itemized the preponderant waveforms as emanating from

- Joint spacing 15ft
- Stringlines ((25ft)
- Multiples especially 2 times the Stringline internodal spacing (50 ft)

According to Wilde Izevbekhai & Krause (5) regardless of the random profile generated, as long as it was generated with the same input parameters to the random profile generator, the variability of the ride statistics were very small for both the IRI and PI. It is concluded in consequence that the percentage increase due to a waveform superposed on the profile is not arbitrary even if the general process of profile generation appears to be. It is important to note that multiple random profiles, generated with the same input parameters, produce profiles with very similar ride statistics. There are predictable changes in the ride statistic when certain features are added to the random profile. The 15-foot (4.6-m) wavelength content added to the random profiles caused large increases in IRI when compared to the random profile (more than double), and the PI 0.0 statistic increased only about 70%. Changes in the ride statistics due to catenary effects on the unmodified random profile were thus

accentuated. The 15-foot (4.6-m) wavelength has the largest impact on IRI and that the combination of the 15- and 25-foot (4.6-m and 7.6-m) wavelengths has the largest impact on PI. $4.1 \text{ in/mi} = 0.0158 \text{ m/km}$, Wilde, Izevbekhai, and Krause (5) also obtained the following results from their analysis

- Random+15-ft upward catenary 104%
- Random+15-ft downward catenary 106%
- Random+15-ft sine wave 115%
- Random+25-ft upward catenary 21%
- Random+25-ft sine wave 22%
- Random+50-ft upward catenary 9%
- Random+50-ft sine wave 9% -3%
- Random+15-ft and 25-ft upward catenaries 118% Increase over Random

Wilde Izevbekhai and Krause (5) also discussed the effect of added wavelengths on IRI and PI. A second analysis was conducted to determine the effects of specific, individual wavelengths on ride statistics. Based on the very small variation in ride statistics between the five random profiles, this second analysis was only conducted using one of the random profiles. Figure 5 shows this sensitivity of IRI and $PI_{0,0}$ to individually added wavelengths. The subscript refers to the zero blanking band. The analysis conducted added a sine wave of the specified wavelength to one of the random profiles used in the previous analysis. Perera et al (6) showed the IRI and PI gain algorithm as in figures 3.2 and 3.3. Evident in figure 3.1 (5) is the respective response of PI and IRI with the 25 ft wavelength addition causing increase in PI of 60% and 20%. The multiplier algorithm in figures 3.2 and 3.3 respectively for IRI and Ride number (which is same for PI) show a gain factor of 0.5 in IRI and 0.1 in PI or RN.

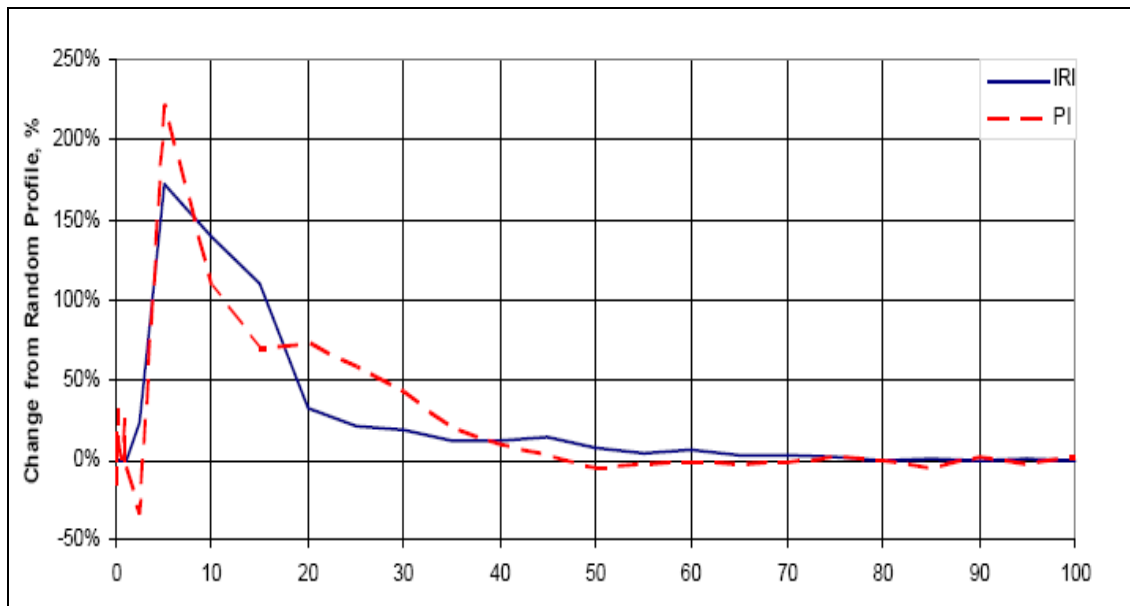


Figure 3.1 Response and of IRI model to added frequency Figure 6: (After Wilde, Izevbekhai & Krause)

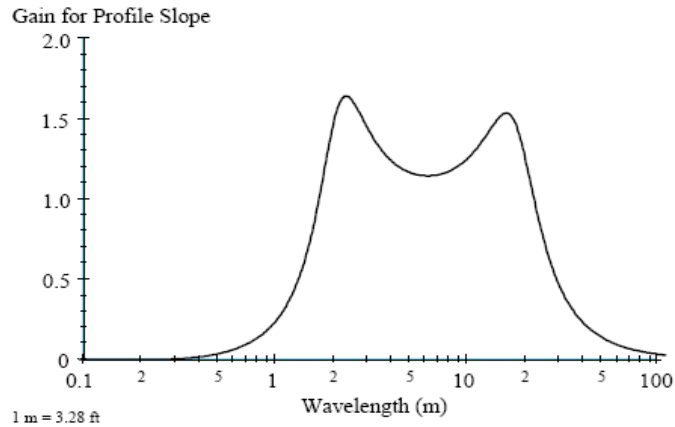


Figure 3.2 Gain Algorithm for IRI (6)

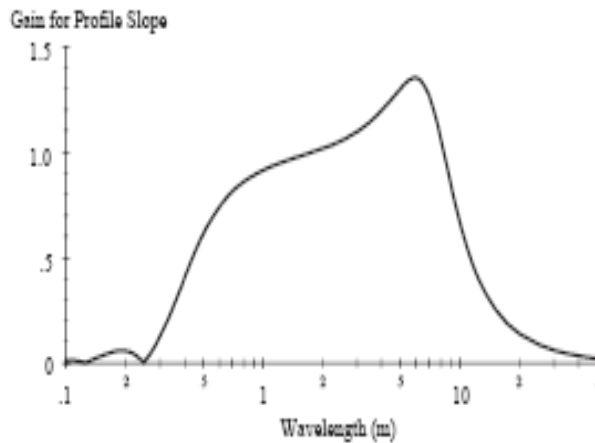


Figure 3.3 Gain Algorithm for PI or RN (6)

Byrum R C (7). discussed :”Slab Curvature Detection In LTPP High-Speed Profilers, Developing Predictive Models Using Generic Non-Linear Optimization”. In their paper, Byrum idealized slab curvature and analyzed their effect on international roughness index. For any constant magnitude of slab curvature, IRI increases exponentially with increasing slab length. Therefore, two pavement sections, one with short joints and one with long joints, constructed in the same way under the same environmental conditions could have significantly different initial IRI values if slab curvature develops. This would not be the result of the contractor’s actions, but is the result of a design decision put in place long before construction. This joint spacing effect should be considered in initial smoothness specifications having very high smoothness requirements that can be affected by typical

locked in slab curvature values. He (7) also observed differences in Maximum slab curvature from wheel path curvature. A road profiler moving at high speeds is measuring the “wheel path view” of slab curvature. The curvature measured along a wheel path is a subdued and distorted image of the maximum slab curvature.

According to Awashti and Singh (8), in their paper “On Pavement Roughness Indices” the simulated profile (profilograms) can be expressed in the series

$$F(x) = (\sigma)(2/N)^{1/2} \sum_{k=1}^{\infty} \cos wkt \quad 3.1$$

considering a Gaussian random process $f(x)$ with mean zero and the spectral density function $S(\omega)$. This process can be simulated by the way of the series.

Area under the PSD curve increases linearly as roughness increases

$$\text{Where } \sigma = \int_{-\infty}^{+\infty} s(w)dw \quad 3.2$$

According to Awashti et al,(7) the PSD value (G_k) at any point k is given as

$$X_k = \sum_{i=1}^{N-1} X_i e^{(-2\pi ik/N)} \quad 3.3$$

$$G_k = 2y/N * (\text{ABS } X_k)^2 \quad 3.4$$

and $w_k(k=1,2,\dots,N)$ are random variables identically distributed by the density function $S(w)$ and represents the PSD curve of the road profile, where y is sample interval; N , total number of sample points; and X_k , the Fourier transformation of the sample points up to k , k being any point.

Figures 3.4 and 3.5 respectively show the stringline supported at 25 ft interval.



Figure 3.4 : Stringlines at 25 ft Interval. This is Typical



Figure 3.5: Stringlines In Close-Up

4 REVIEWER’S VALIDATION OF EFFECTS OF STRINGLINE ON PAVEMENT PROFILE

In this section Reviewer validates effect of stringlines by going through the process set forth in NCHRP 335 appendix E (11) and reported by authors (1). This section studies the effect of stringline on vertical curve to accentuate the chord effect identified by Rassmussen et al (1), the following process was utilized.

Step 1: A field value of a vertical curve was generated, using the approach slope of 0.5 and the exit slope of -0.6. Using an interval of 0.1ft, the vertical curve was generated. The formula used was g_1X
The formula used was

$$E + g_1X + (g_2 - g_1) X^2 / 2L \dots\dots\dots 4.1$$

- Where E is the datum elevation
- g_1 is approach slope
- X is station with respect to the Cove
- g_2 is the departure slope
- L is the length of curve

Step 2 . Similar curves were generated for the

- vertical curve with stringlines and for the
- vertical curve without stringline

For sag of 0.1ft, the Stringline catenary is idealized to be

$$F(x) = 0.1 - SG * (ABS(SIN(3.14157 * X / INT)))) \dots\dots\dots 4.2$$

- Where SG is the maximum sag due to loose stringlines
- (SG is sag of the stringline
- ABS (SIN(3.14157 *
- X is the station
- INT is stringline support interval.

The profile formed from equation 4.2 is a survey profile and not a ride profile. To convert it to a ride profile we need to know how the quarter car will respond to that profile. The response profile of the quarter car is the ride profile. This leads to the next step.

Step 3: Each of the 3 Profiles were exported into the raw ProVAL software and the resulting ASCII file was saved as ERD files. The resulting Profile was analyzed for ride quality, PSD and ride statistics. The resulting profiles and intrinsic properties are shown in figures 4.3 and 4.4.

Table 4.1 Vertical Curve Example

E _{one} =0			INT=25	g _{one} =-0.5		EI=500 g ₂ = -0.6	500
	VC	STR	VC +STR		VC	STR	VC +STR
0	0	0.1	0.1	1.3	-0.64814	0.083736	-0.5644
0.1	-0.04999	0.098743	0.048754	1.4	-0.69784	0.082498	-0.61535
0.2	-0.09996	0.097487	-0.00247	1.5	-0.74753	0.081262	-0.66626
0.3	-0.1499	0.096231	-0.05367	1.6	-0.79718	0.080029	-0.71715
0.4	-0.19982	0.094976	-0.10485	1.7	-0.84682	0.078799	-0.76802
0.5	-0.24973	0.093721	-0.156	1.8	-0.89644	0.077573	-0.81886
0.6	-0.2996	0.092467	-0.20714	1.9	-0.94603	0.07635	-0.86968
0.7	-0.34946	0.091215	-0.25825	2	-0.9956	0.075131	-0.92047
0.8	-0.3993	0.089964	-0.30933	2.1	-1.04515	0.073916	-0.97123
0.9	-0.44911	0.088714	-0.36039	2.2	-1.09468	0.072705	-1.02197
1	-0.4989	0.087467	-0.41143	2.3	-1.14418	0.071498	-1.07268
1.2	-0.59842	0.084978	-0.51344				

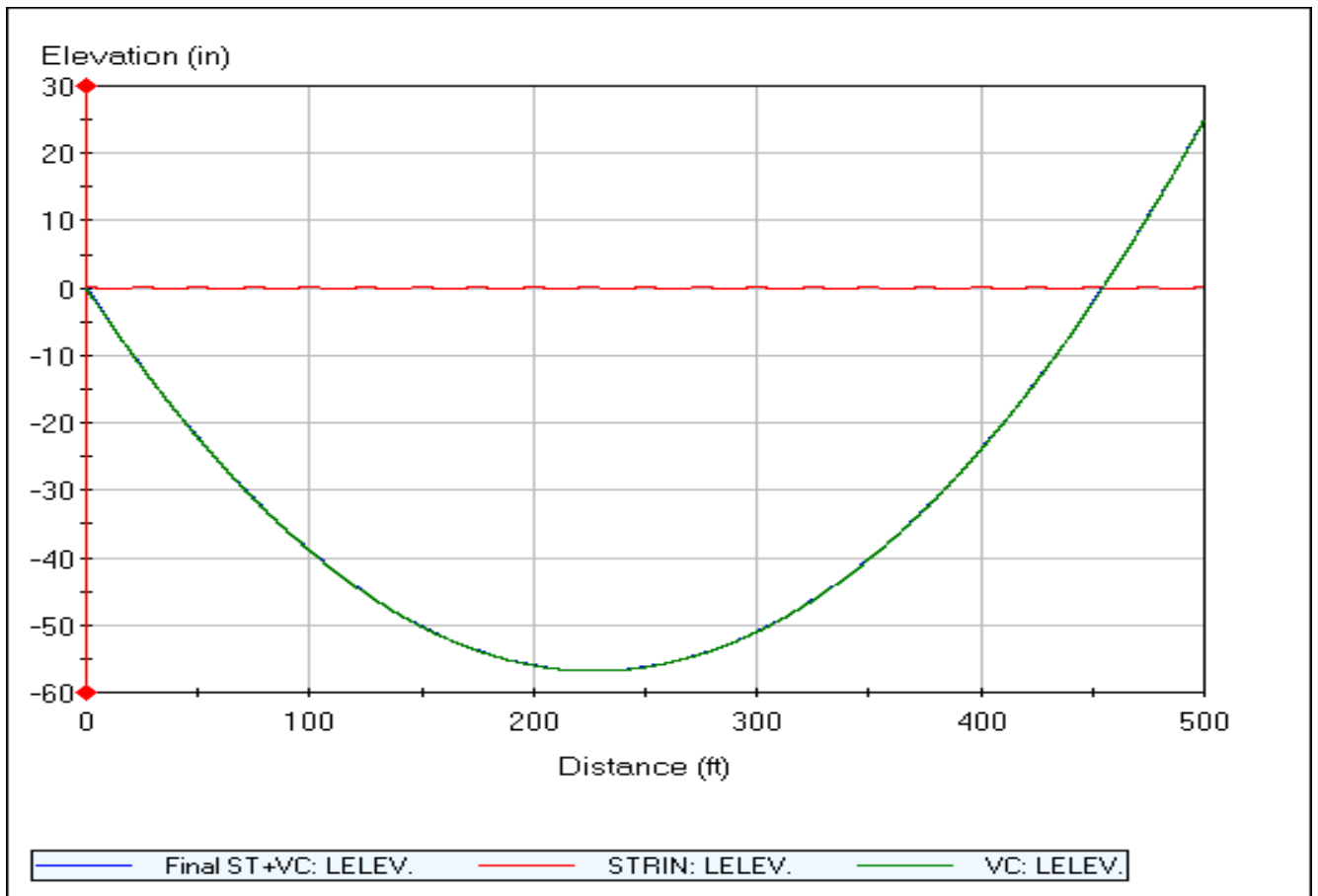


Figure 4.3: Analysis of Stringline Chord Effect Using ProVAL Software

Table 4.2: Analysis - Ride Statistics

Channel Title	IRI (in/mi)	PTRN (in/mi)	RN
Stringline	45.5	51.7	4.39
Vertical Curve	8.9	24.5	4.70
String Line Imposed on Vertical Curve	49.6	59.7	4.30

Input	Value	Unit
PSD Calculation	Slope	
Use Point Reset	No	
Frequency Averaging	No	
Constant Frequency Interval	0.003048	cycle/ft
Pre-Processor Filter	None	

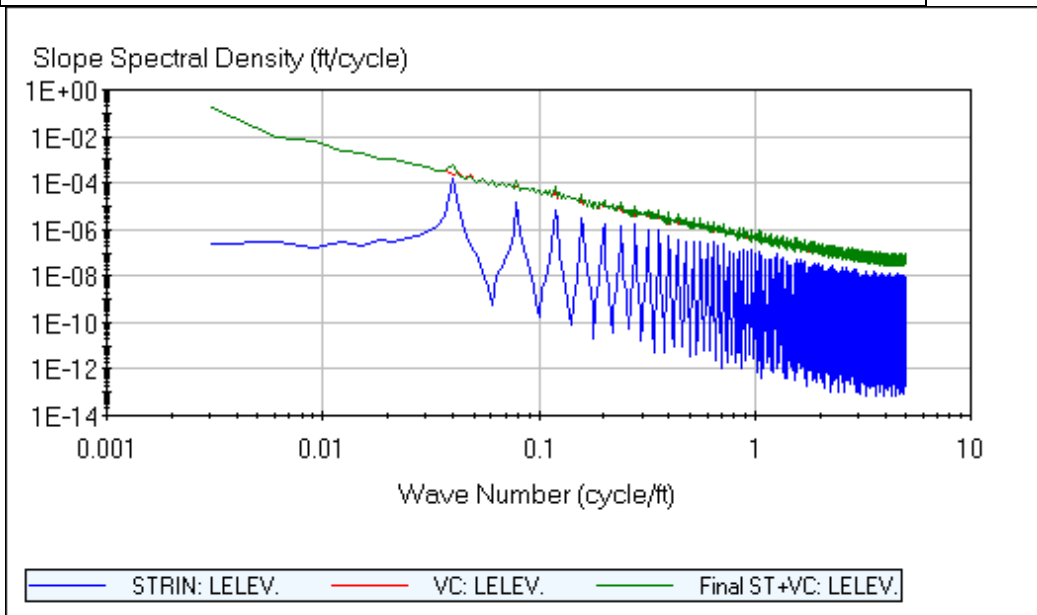


Figure 4.3: PSD of Stringline Showing the highest harmonics at 25 ft wavelength

Generation of pavement surface is a common feature in pavement profilometry. The output obtained provides information to a pavement designer who can minimize the effects of certain resonant frequencies by providing adequate joint spacing, avoiding “finising-pan”-induced sinusoids and ensuring tight stringlines as well as minimizing survey errors.

To convert a profile from the spatial to the frequency domain, the following process is required is required

$$F(x) = a_n \sum \sin \omega x + \sum b_n \sum \cos \omega x \dots\dots\dots 4.1$$

for all aperiodic signals (9)

Where $f(x)$ is the profile and a_n and b_n must be determined

$$\begin{aligned}
 f(x) &= a_0/2 + \sum_{n=1}^{\infty} a_n \cos n\pi x/L + \sum_{n=1}^{\infty} b_n \sin n\pi x/L \\
 &= a_0/2 + a_1 \cos \pi x/L + a_2 \cos 2\pi x/L + a_3 \cos 3\pi x/L + \dots \\
 &\quad + b_1 \sin \pi x/L + b_2 \sin 2\pi x/L + b_3 \sin 3\pi x/L + \dots
 \end{aligned}
 \tag{4.3}$$

$$X_i = \sum_{n=0}^{N-1} a_n \cos (\nu 2\pi i/N) + b_n \sin (\nu 2\pi i/N) \dots\dots\dots(4.4)$$

Where a_n and b_n are fourier coefficients $0 \leq \nu \leq N/2$
 x_i is the profile elevation

Consequently

$$a_n = 1/N \sum_{i=0}^{N-1} x_i \cos (\nu 2\pi i/N)$$

$$b_n = 1/N \sum_{i=0}^{N-1} x_i \sin (\nu 2\pi i/N)$$

$w(\nu) = \nu / (N\Delta t)$ where

where $w(\nu)$ is the frequency corresponding to ν and Δt is the sampling interval

It can therefore be proven that removal of highly amplified wavelengths will improve pavement smoothness.

N is number of profile elevation data points

The amplitudes represent maximum warp or maximum stringline sag. Evidently the degree of sag in a truly truncated or normalized sine wave in which

$$f_x = \text{Abs} (\text{Sag} * \text{Sin} (\pi x / 25)) \dots\dots\dots(4.5)$$

The process and effect of addition of wavelengths on a randomly generated profile (11) are shown in appendix C and exemplified in section 5.

5 CASE STUDY OF A TYPICAL PAVEMENT EXHIBITING CHATTER PHENOMENA

A largely biased set of data has been chosen for this project. This is the data from Minnesota Highway 59 in Morris. Reviewer ran a lightweight profiler on this project in 2004 in response to complaints that the section was riding poorly. Riders experienced the “Chatter Phenomenon” on that pavement. The ERD files were analyzed in PSD and the dominant wavelengths stood out at 25 ft, 15 ft and 7.5ft. This is shown in figures 5.1 and 5.2. In this section, the TH 59 ride files are analyzed for the preponderant wavelength. A theoretical warp and curl profilogram and stringline profile were generated and compared to the actual IRI measured. In this exercise, the initial model was investigated in the spatial domain. Subsequently, a Fourier transform of the elevation data was done and the moduli of each data point in the Stringline, warp-and-curl as well as Synergistic waveforms at 75 ft wavelength. "Warp" is a temperature dependent curvature of slabs caused by a temperature gradient in a concrete slab. When the top temperature exceeds the bottom, the curvature of the top fiber exceeds the bottom. When this phenomenon occurs in the early stage of strength the gain, built in curl & warp are created in the profile.

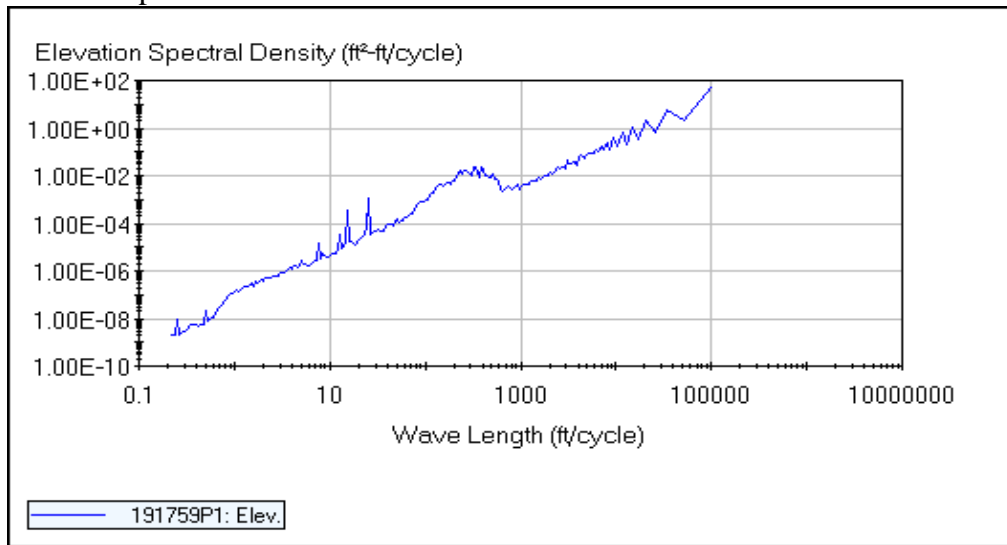


Figure 5.1 Dominant frequencies from a PSD on the ride Files from Highway 59

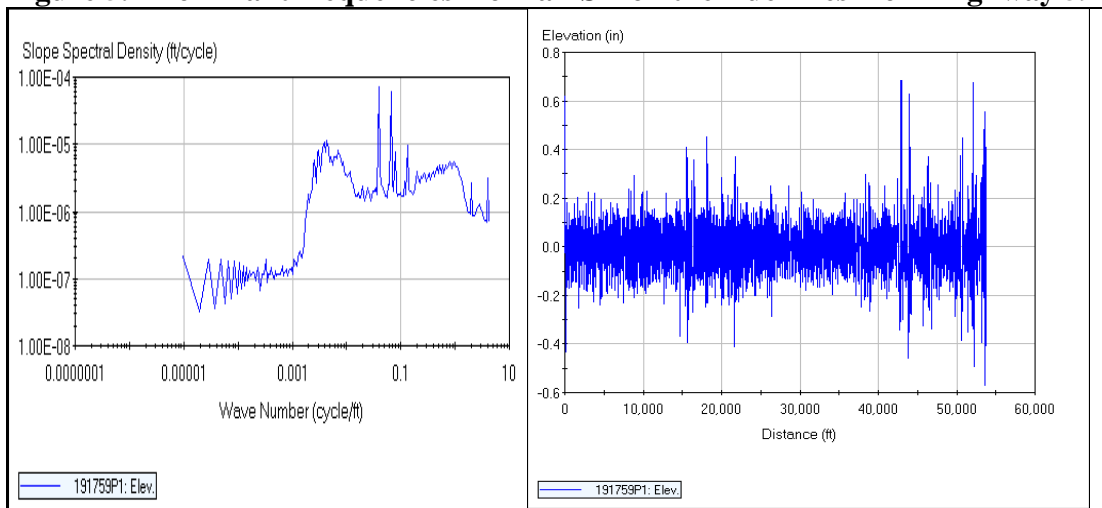


Figure 5.2 PSD and Profilogram on US TH 59

Table 5.1 Reviewer’s Generation of Components of the TH 59 Ride Phenomena (Joints, Stringlines, Synergistic) An Excerpt from 55000 rows

Alpha=	0.1				
Beta=	0.1				
Ceta=	0.15				
191759P2 - 0.0 to 5380.0 ft: Elev.					
Distance (ft)	Total EI	IRI _J	IRI _{SEL}	IRI _{CEL}	Synthetic
0	-0.5664	0	0	0	-0.5664
0.1	-0.5664	0.002093	-0.00063	-0.00063	-0.56724
0.2	-0.5713	0.004185	-0.00126	-0.00126	-0.57297
0.3	-0.5664	0.006276	-0.00188	-0.00188	-0.56891
0.4	-0.5664	0.008364	-0.00251	-0.00251	-0.56974
0.5	-0.5713	0.010448	-0.00314	-0.00314	-0.57547
0.6	-0.5713	0.012527	-0.00377	-0.00377	-0.57629
0.7	-0.5762	0.014601	-0.0044	-0.0044	-0.58201
0.8	-0.5713	0.016668	-0.00502	-0.00502	-0.57792
0.9	-0.5664	0.018729	-0.00565	-0.00565	-0.57383
1	-0.5664	0.020781	-0.00628	-0.00628	-0.57462
1.1	-0.5615	0.022824	-0.00691	-0.00691	-0.57051
	-				
1.2	0.5566	0.024857	-0.00753	-0.00753	-0.56639
	-				
1.3	0.5566	0.026879	-0.00816	-0.00816	-0.56716

Table 5.2: Reviewer’s Fourier Transforms and Component Moduli of Joints, Stringlines and Synergistic Phenomena

X	Total Modulus	Joints modulus	Stringline Modulus	Synergy Modulus	Synthetic Modulus
0.00000	666.877200	259.804543	259.661720	389.383218	277.636806
0.10000	289.447230	0.957614	1.117202	3.400944	288.650964
0.20000	218.706644	0.968232	1.176178	6.724176	211.781542
0.30000	894.921594	0.978545	1.270885	12.167349	882.373882
0.40000	91.531047	0.998200	1.404773	24.154089	80.733617
0.50000	198.117654	1.022177	1.577574	86.113796	117.816452
0.60000	245.998715	1.053326	1.794885	79.245149	319.874879
0.70000	172.234203	1.090366	2.064623	29.598841	200.120675
0.80000	55.924929	1.134978	2.402035	18.776047	63.998417
0.90000	96.807098	1.187052	2.830803	13.886285	108.618789
1.00000	91.653221	1.248120	3.392018	11.012673	99.663294
1.10000	89.809076	1.318926	4.156989	29.212067	107.738462
1.20000	60.410447	1.401363	5.264674	8.581472	65.609368
1.30000	119.426381	1.497226	7.017134	7.059681	119.688133
1.40000	81.966725	1.609365	10.229369	5.825033	83.561033
1.50000	92.193267	1.741307	18.078176	4.301473	79.290913
1.60000	82.519730	1.897990	67.602404	4.079991	140.343066
1.70000	65.637778	2.086369	41.454147	10.428722	103.306679
1.80000	31.530174	2.316171	16.200458	6.870290	56.295796
1.90000	39.201351	2.602359	10.175435	5.755683	57.086791
2.00000	54.125516	2.967314	7.459666	5.048835	68.033036

5.2 Simulation of Actual Warp or joint Phenomena

For the purpose of this project, a sinusoid of warp is created with the following equation.

$$Y_x = \text{WARP}_{\max} \cdot \text{ABS}(\text{Sin } \pi x/15) \dots \dots \dots 5.1$$

This equation represents the approximate profile of a warped slab. To subtract the effect of a warped slab; the ERD file must be reconverted into a text file that shows only the curvature. Elevation records are taken every 0.1' although the laser sweeps continuously. Pseudo-sinusoids are then subtracted from the ASCII profilogram to generate a new profilogram, which has to be analyzed again with the IRI algorithm to recreate a new ERD file from which the new IRI is read off. In that way the ride quality resulting from the absence of the warp can be quantified.

5.3 Simulation of String line

This is similar to the effect of Joints except that the catenary will account for be defined by the simple equation based on a 25 ft string-line. To simulate catenary from tensioning forces properties of the cable have to be known. The grip and anchorage methods have to be reliable enough for the applicable equations to be used. However, it can be simulated into a sine or cosine wave

$$Y_x = \text{SG}_{\max} \text{ABS}(\text{Sin } \pi x/25) \dots \dots \dots 5.2$$

A better simulation was found in

$$Y_x = \text{SG}_{\max} (1 - \text{ABS}(\text{Cos } \pi x/25)) \dots \dots \dots 5.3$$

5.4 Data Processing

To process this data, the ERD files were opened in ASCII format. This lists the elevation at every 0.1 ft although the laser records continuously. Ride statistics every 75ft waveform will be Synergistic as for joints & string-line as this is the least common multiple of 15 and 25. Occasionally, multiples of critical wavelength, 30-ft, and 50-ft are detected by the PSD analysis when intermediate joints are locked.

A better model was obtained by performing a Fourier transform on the components and modeling the component parameters. In that case the moduli of each component was modeled. An excerpt of the Moduli table is shown in table 5.2. Reviewer determined C_1 C_2 and C_3 C_4 and C_5 Using the Marquardt-Levenberg-Technique. Figure 5.4 a, b and c show the results of this process.

Wavelength range at which different roughness parameters are most sensitive are different for different indices. Hence, no definite conclusion can be drawn regarding relative efficiency of various indices as a close representative of rider comfort. Very small wavelengths do not contribute to road roughness as the vehicle tires are too wide for these wavelengths to register any vibration. Very large wavelengths are not perceived by the vehicles at all. Pavement engineers need to know what wavelength range actually contributes to the road roughness. The roughness index can be derived from elevation profile, slope profile or the acceleration profile. When elevation profile is used as roughness index, it is found that, if short wavelengths are removed from the profile, there is almost no effect, but if large wavelength are removed, there is a tremendous decrease in the roughness level. In case of slope profile defined as roughness, there is a reduction in the level of roughness if either of the two large or short wavelengths are removed. For acceleration profile, on the other hand, if long wavelengths are removed the effect is little, but removal of short wavelengths causes appreciable reduction in the level of roughness. Any roughness index if well defined must include the range of actively influential frequencies, the filter algorithms as well as the testing speed or rate of data acquisition .

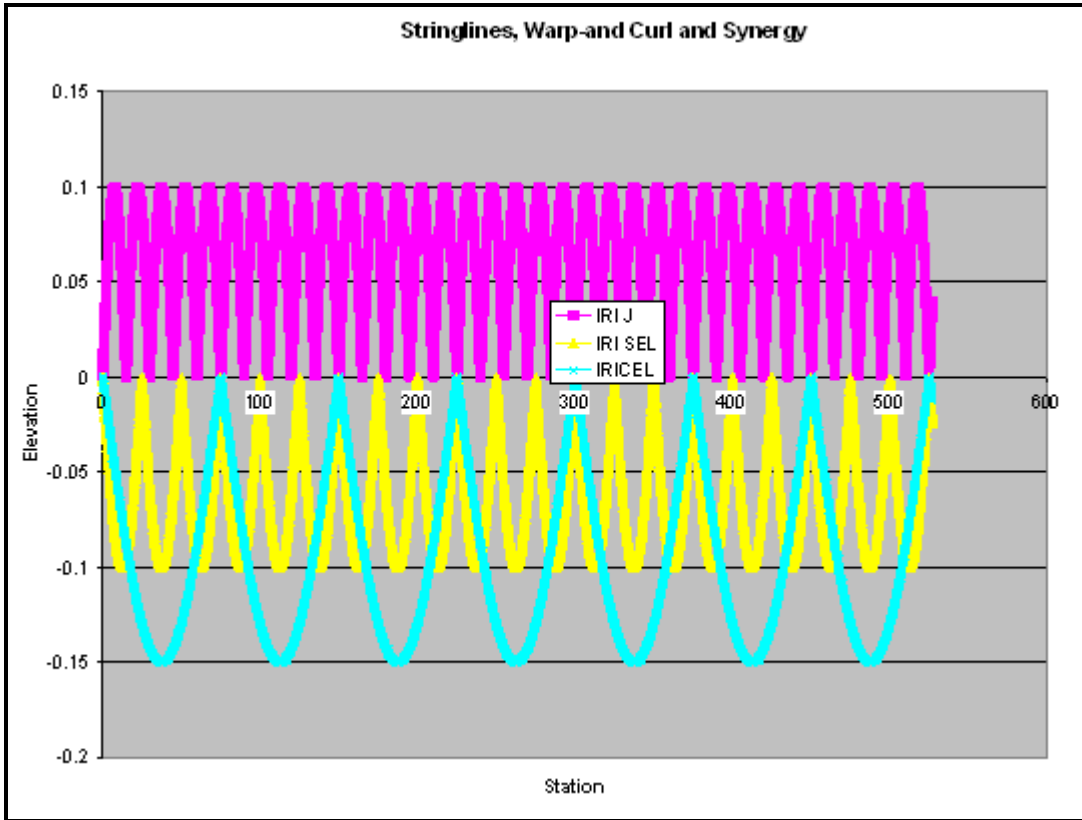


Figure 5.3: Simulation of Warp and String line errors in Concrete surface Profile

5.5 Model Fitting (The Initially Proposed Model)

Non linear model Using Levenberg- Marquardt

Let C_1 = effect of Curl IRI_{curl}

Let C_2 = effect of String line IRI_{curl}

Let C_3 = Effect of a collection of Other Roughness sources

X_1 is parameter 1

X_2 is parameter 2

A generic equation will take the form

$$\begin{aligned}
 F(X_1, X_2, C_2, C_3) &= C_3 \exp(C_1 X_1^2 + C_2 X_2^2) \\
 \partial f / \partial C_1 &= X_1^2 C_3 \exp(C_1 X_1^2 + C_2 X_2^2) \\
 \partial f / \partial C_2 &= X_2^2 C_3 \exp(C_1 X_1^2 + C_2 X_2^2) \\
 \partial f / \partial C_3 &= X_3^2 C_3 \exp(C_1 X_1^2 + C_1 X_1^2) \dots \dots \dots (5.7)
 \end{aligned}$$

The Initial Model is

$$IRI_{total} = C_4 \exp(-C_1 IRI_j * C_2 IRI_{str} * C_3 IRI_{syg}) + C_5 \dots \dots \dots (5.8)$$

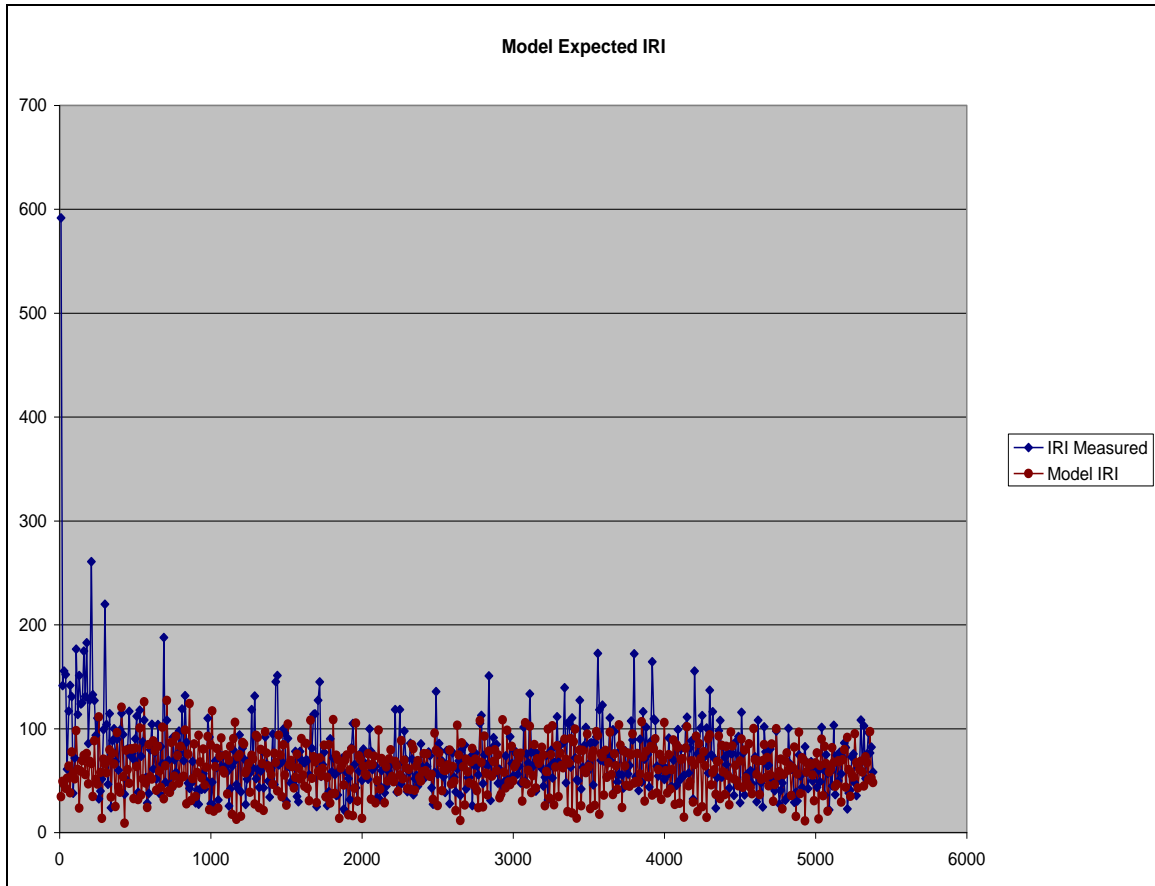


Figure 5.4a Model based on component frequencies versus measured IRI

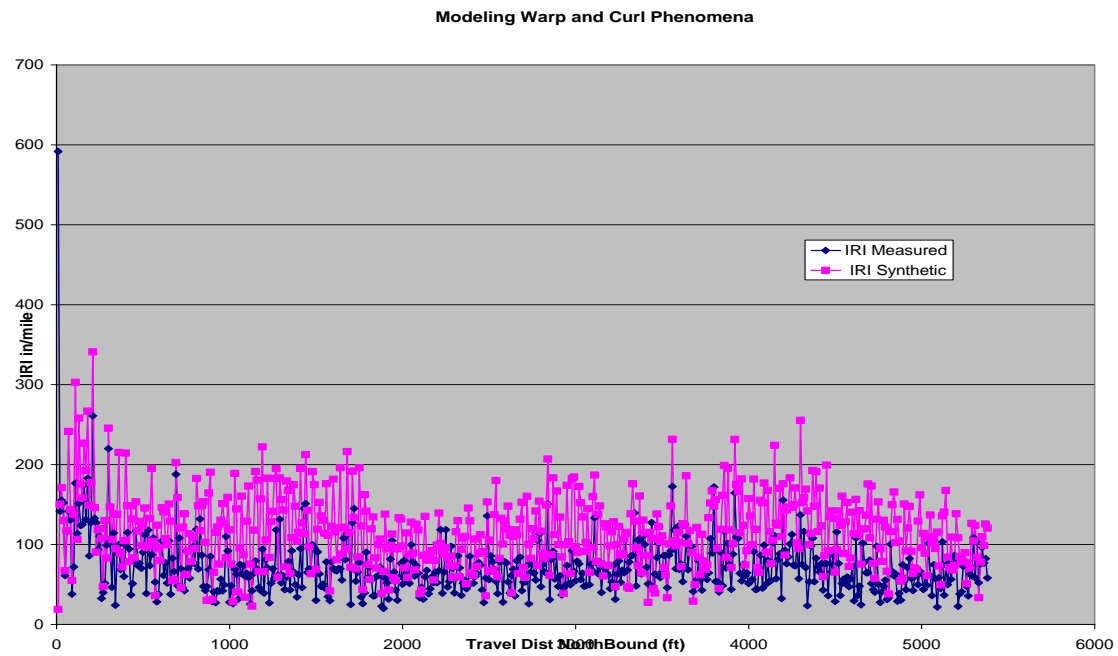


Figure 5.4 b Model Versus measured IRI

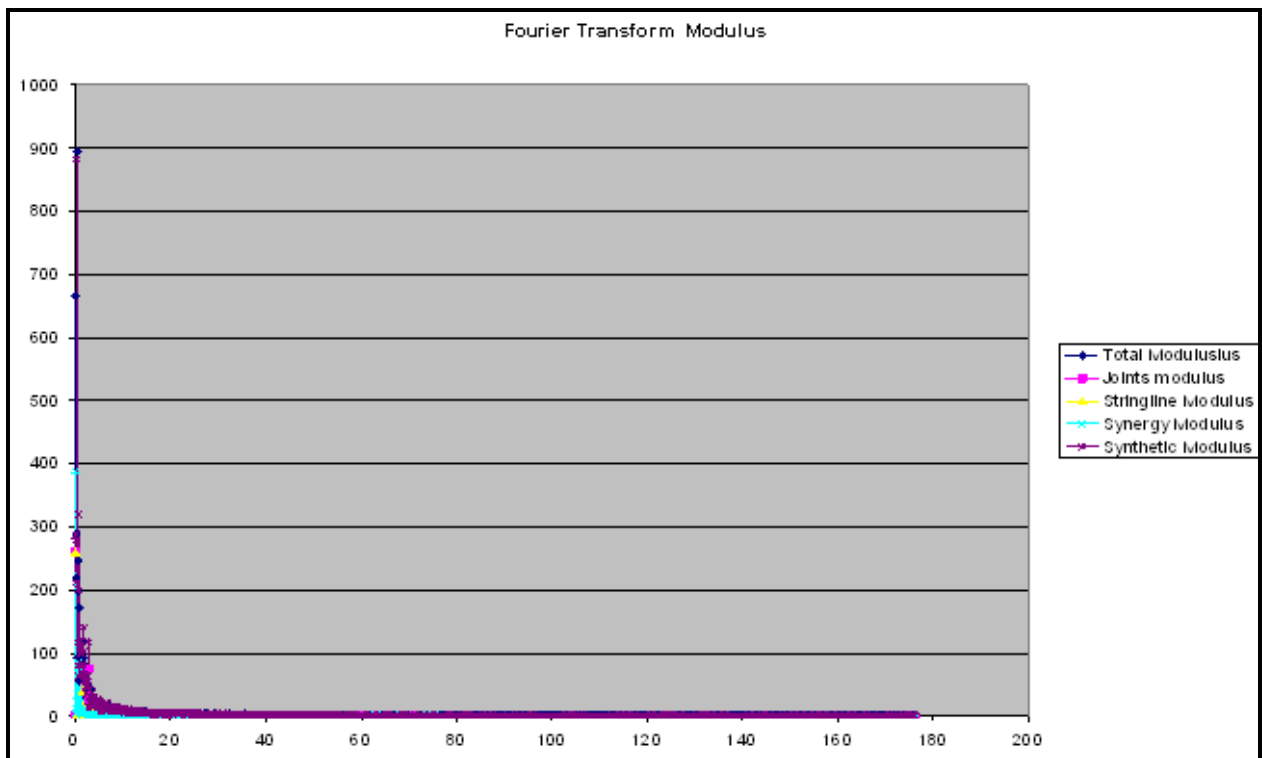


Figure 5.4C: Model of Moduli from Fourier Transform

Table 5.3: Correlation of Fourier Transformed Profilogram Elevations

	<i>X</i>	<i>Total Modulus</i>	<i>Joints modulus</i>	<i>Stringline Modulus</i>	<i>Synergy Modulus</i>	<i>Synthetic Modulus</i>
<i>X</i>	1					
<i>Total Modulus</i>	0.106113638	1				
<i>Joints modulus</i>	-0.05689813	0.526784844	1			
<i>Stringline Modulus</i>	-0.05956888	0.551298631	0.909642821	1		
<i>Synergy Modulus</i>	0.060268391	0.628259996	0.906164402	0.914550961	1	
<i>Synthetic Modulus</i>	0.119439849	0.943934993	0.284954513	0.313220477	0.380388881	1

There is a strong correlation between the synthesized profilogram elevation and the profilograms due to preponderant waveform. This was expected as the generated profilograms was taken as the elevation of originals profile the sum of elevation from the influential wavelengths thus indicating that the chosen preponderant frequencies are influential to IRI of the section. However, the spectra of each of the 3 influential wavelengths were moderately correlated to that of original section original section. Moduli obtained from Fourier transform, and plotted against distance showed a decay curve as in figure 5.4c. Evidently, a curve fitting of the moduli from the fourier transform resulted in a better correlation than that of the Spatial domain.

The fitted curve had the following function

$$\begin{aligned}
 \text{IRI Generated} = & (\text{IRI}_{\text{joi}} * \text{alpat} * \text{ABS}(\text{SIN}((2 * 3.142 * X / \text{kjoi}) + \text{phijoi})) + \\
 & (\text{betat} * \text{IRI}_{\text{Str}} * \text{ABS}(\text{SIN}((2 * 3.142 * X / \text{kstr}) + \text{phistr}))) + \\
 & (\text{IRI}_{\text{Syn}} * \text{cetat} * \text{ABS}(\text{SIN}((2 * 3.142 * X / \text{ksyn}) + \text{phisyn})))) * 200 \dots \dots \dots (5.4)
 \end{aligned}$$

Alpat, Betat and Cetat are the hypothetical arithmetic Max (Mid Panel or midspan warp/curl),

- Zeta 12
- alpat= 0.003594
- betat= 0.001876
- cetat= 0.006276
- Kjoi= 14.95268 Phi joi -4.75245
- Kstr= 24.93694 Phistr 1.849599
- Ksyn= 74.05236 Phisyn 1.339196

Stringline sag and synergistic hump if all panels or group of panels in the section are affected. Kjoi, Kstr, Ksyn are respective joint, stringline and Synergy constants that relate to their actual wavelengths. The model actually picked them up as the were not forced into the solution by the reviewer. Phijoi, Phistr and Pohisyn are the respective phase angles. Zeta is a constant that bears no recognizable physical property at the moment.

Model recognizes preponderant wavelengths. Further work will utilize peak picking and analysis of intermediate harmonics towards a better model. Effects of warp and curl have been quantified in the spatial and spectral domain.

It is pertinent to explain the real meaning of power spectral density in terms of ride quality. Simulated profile or profilograms is given by According to Awashti and Singh (8), are shown in equations 3.3 to 3.4.

Authors (1) did not explain the implications of a 25 ft or 50 ft rhythm at a freeway speed on the human tolerance. Ultimately when a pavement feature causes roughness, it is the response of the rider that matters.

The human body exhibits minimum tolerance to vertical vibration at about 5 Hz due to resonance of the abdominal cavity. Duration of vibration defines the amount of time a person is in contact with the vibrating object and human response to vibration increases with the increase in duration of exposure. Vibration is normally measured along three orthogonal axes, as the human body reacts differently to different direction of vibration. Studies have found that Roughness Indices, such as, IRI, and RN are somewhat unrelated to the parameters indicating the level of human discomfort. However, it is observed that human judgment on roughness discomfort is most susceptible within the wavelength range between 0.5 m to 2.5 m 1.5 ft to 7 ft approximately. Judgment of the roughness level by a road user mainly depends on the vibration discomfort of the ride experienced while using the road. Severity of vibration caused to human body is determined by its magnitude, frequency, duration and direction. Magnitude is measured in terms of the acceleration of oscillating particles and is expressed as a root mean square value. Each part of human body has its own natural frequency of vibration, therefore, the extent to which the human body is affected depends on the vibration frequency it is exposed to The human body is more sensitive to vibration in some frequency ranges than in others.

6 CONCLUSIVE REMARKS

This reviews the paper titled Effects of stringline on Concrete pavement construction, Published by the Transportation Research Journal, Transportation Research Record 2000 Issue Number: 1900 of 2000.

- Reviewer elucidated the metrics for ride quality measurement as well as their gain algorithms in relation to dominant wavelength and validates that stringlines affect initial ride quality of concrete pavements. A vertical curve of 500 ft long and 20 ft deep with an approach gradient of 5% and an exit gradient of -6% caused a 9% increase in pavement roughness, thus corroborating the factorials performed by the authors and their inference on the effects of stringlines.
- This review validates both analytically and practically that stringlines do have pronounced effect on ride quality. In the analytical process, a vertical curve and a stringline profile were generated, combined and subjected to the IRI algorithm. The result showed a percentage increase in roughness due to the imposition of a profilogram from a stringline catenary. The

dominant wavelengths of a true project profilogram were analyzed and a curve of measured versus computed IRI was fitted.

- By generating the IRI of a concrete pavement with 15 ft joint spacing, the IRI per 0.1ft of warp was 77.8 inches per mile. In a similar analysis for a stringline of 25 ft support interval, the IRI per 0.1 ft of sag was found to be 44.5 inches per/mile. Similarly, the synergistic effect occurring at 75 ft, (First true multiple of 25 and 15) was found to be 14.8 inches per mile. Though the IRI computed per sag or curl is linear, the theorem assumes that all panels are warped (or curled) and all stringline spans are sagged. By implication, for a percentage of affected slabs the resulting IRI is in direct proportion to the computed total. This observation is important in pavement management.
- A better prediction model of the measured IRI was obtained by performing a Fourier Transform and fitting the moduli of the 3 isolated dominant wavelengths from stringlines, joints and a synergistic combination of both to that of the measured IRI.
- Although Stringlines affect initial ride quality of pavements, features such as built-in warp and curl occur after paving. In addition to stringline-induced roughness, there should be prediction models for post paving warp and curl based on mix design, placement temperature, humidity, evaporation rate, joint spacing and admixtures. Otherwise it is advisable to perform initial ride measurement when built-in warp and curl are deployed.

7 REFERENCES

- 1 Rasmussen, R O; Karamihas, S M; Cape, W R; Chang, G K; Guntert Jr, R M
Stringline Effects on Concrete Pavement Construction
TRB Transportation Research Record 2000 Issue Number: 1900
- 2 Izevbekhai B.I. Optimization of Pavement Smoothness and Surface Texturing in Pavement Infrastructure. Center for the Development of Technological Leadership (CDTL) University of Minnesota 2004.
- 3 Sayers, M, W, Karamihas, S.K. Little book on Profiling University of Michigan Transportation Research Institute UMTRI . 1998.
- 4 Smith K.L, Smith, K.D., Evans L.D., Hoerner, T.E, Darter , M.I. “Smoothness Specification for Pavements” Final Report NCHRP 1-31 March 1997. NCHRP, TRB, NRC
- 5 Wilde W. J., Izevbekhai, B.I., and Krause, M.H. Comparison of Profile Index and International Roughness Index in Payment of Incentives in Pavement Construction TRB (2007) Transportation Research Records

- 6 R.W. Perera, S.D. Kohn, and S. Tayabji. Achieving a High Level of Smoothness in Concrete Pavements Without Sacrificing Long-Term Performance DTFH61-01-C-00030 FHWA-HRT-05-068 Federal Highway Administration 6300 Georgetown Pike McLean, VA 22101-2296.
- 7 Byrum R Christopher. Slab Curvature Detection In LTPP High-Speed Profiles; Developing Predictive Models Using Generic Non-Linear Optimization Soil And Materials Engineers Inc., Plymouth, Michigan, USA
- 8 Awashti G Singh T Das A On Pavement Roughness Indices
URL <http://www.ieindia.org/publish/cv/0503/may03cv6.pdf> Assessed
April 14 2008
- 9 Papagiannakis, A.T., Raveendan, B International Standards Organization- Compatible Index for Pavement Roughness Paper # 98-0265 Transportation Research Record # 1643 .Pages 110 to 115
- 10 Shubham Rawool And Emmanuel G. Fernando Methodology For Detection Of Defect Locations In Pavement Profile Journal of the transportation Research Board. Transportation Research Board of the National Academies. Volume 1905/2005 Pages 140 to 147 . 0361-1981
- 11 Gillespie , T.D., Karamihas, S.K., Sayers M.W., Nasim, M.A., Hanson W., Ehshan, N. Effects of heavy Vehicle Characteristics on Pavement Response and performance. National Cooperative Highway Research Program Report 353. University of Michigan Transportation Research institute (UMTRI) Ann Arbor Michigan. Transportation Research Board National Academy Press Washington D.C. 1993

APPENDIX A PROVAL CONVERSION PROGRAM

ERDFILEV2.00

1, 10501, 10501, 1, 5, 0.1, -1

TITLE Curled Profile

SHORTNAMLelev.

UNITSNAMin

XLABEL Distance

XUNITS ft

FORMAT (G14.6)

END

0

-0.001255967

-0.002511736

-0.003767108

-0.005021887

-0.006275873

-0.007528869

-0.008780677

-0.010031101

-0.011279942

-0.012527003

-0.013772088

-0.015015001

-0.016255545

-0.017493525

-0.018728745

AppendixB Co_Siter Excerpts

Title: [Sunday, September 07, 2008 2:15:27 PM](#)

Stringline Effects on Concrete Pavement Construction

Journal Transportation Research Record: Journal of the Transportation Research Board

Publisher: Transportation Research Board of the National Academies

ISSN0361-1981

Issue Volume: 1900 / 2004

Category: Materials and Construction

DOI10.3141/1900-01 Pages3-11

Online Date Monday, January 29, 2007

Abstract

Text: Modern concrete pavement construction typically uses slipform paving equipment, especially on major highways and airfields. This equipment commonly is guided by its sensing of a stringline set in advance by an engineering survey. Although use of stringline guidance has improved the smoothness of pavement, some limitations of this technique are known to exist. Three of these limitations are explored in detail. The effects on concrete pavement smoothness from the chord effect, the sag effect, and random survey error are described both conceptually and analytically. Of these three effects, random error introduced during the engineering survey is found to be the most pronounced.

Furthermore, this analysis shows that contradictions exist within what is sometimes considered good practice for concrete pavement construction; the belief that improved smoothness can be obtained by simply using shorter spacing of the stringline stakes is not always correct. In fact, it is demonstrated that optimum stringline spacing can be realized by recognizing each of the effects described, including the associated costs of mitigation.

Authors

Robert Otto Rasmussen¹, Steven M. Karamihas², William R. Cape³, George K. Chang¹, Ronald M. Guntert⁴

¹ Transtec Group, Inc., 1012 East 381/2 Street, Austin, TX 78751

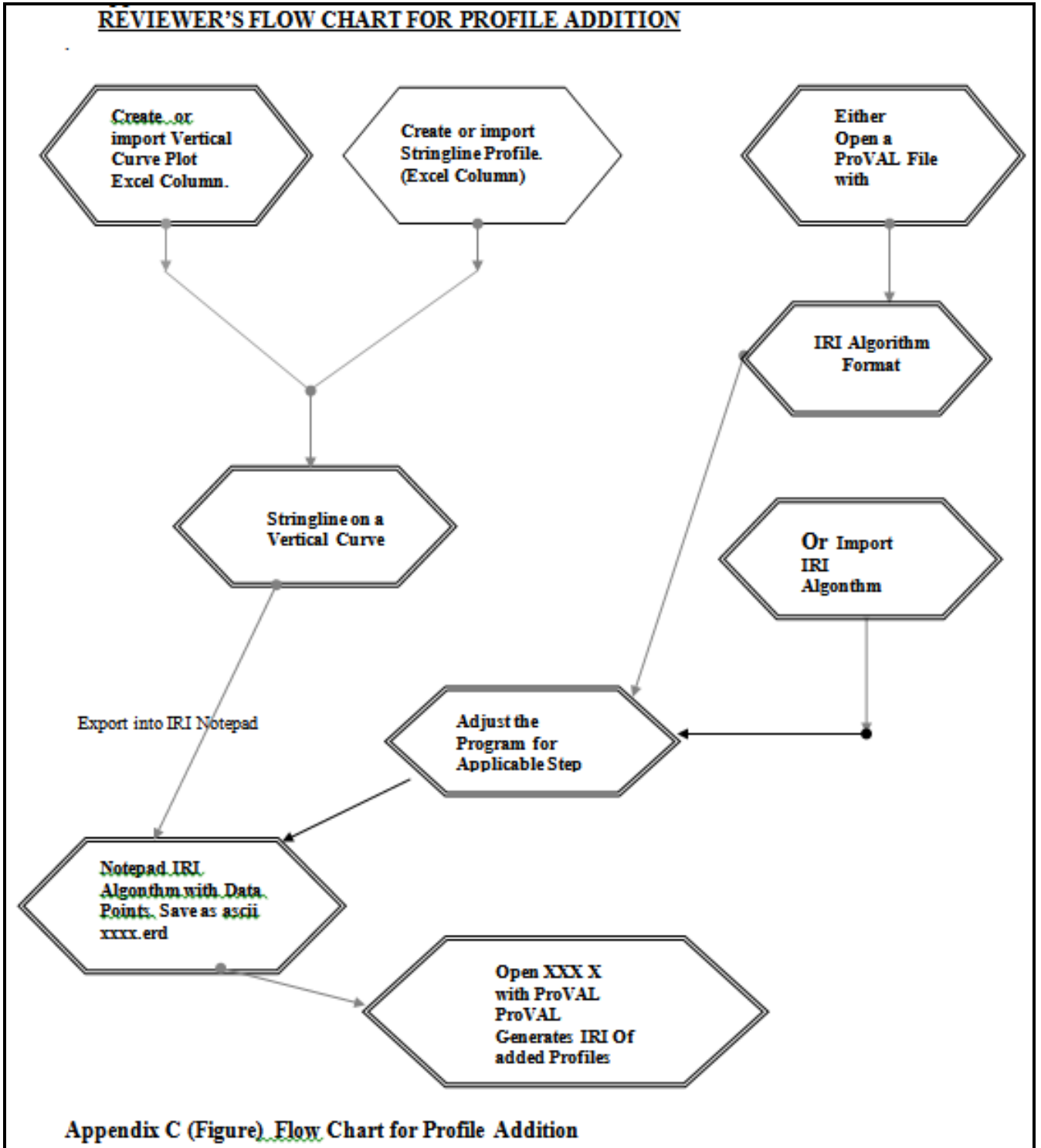
Comment: ² University of Michigan Transportation Research Institute, 2901 Baxter Road, Ann Arbor, MI 48109

³ James Cape & Sons, P.O. Box 044580, Racine, WI 53404-7012

⁴ Guntert & Zimmerman Construction Division, Inc., 222 East Fourth Street, Ripon, CA 95366

From: <http://trb.metapress.com/content/k6461h2350016517/>

Appendix C (Figure) Flow Chart for Profile Addition



Appendix C (Figure) Flow Chart for Profile Addition